

This item is the archived peer-reviewed author-version of:

Identification of ageing state clusters of reclaimed asphalt binders using principal component analysis (PCA) and hierarchical cluster analysis (HCA) based on chemo-rheological parameters

Reference:

Margaritis Alexandros, Soenen Hilde, Franssen Erik, Ppintakos Georgios, Jacobs Geert, Blom Johan, Van den bergh Wim.- Identification of ageing state clusters of reclaimed asphalt binders using principal component analysis (PCA) and hierarchical cluster analysis (HCA) based on chemo-rheological parameters
Construction and building materials - ISSN 0950-0618 - 244(2020), UNSP 118276
Full text (Publisher's DOI): <https://doi.org/10.1016/J.CONBUILDMAT.2020.118276>
To cite this reference: <https://hdl.handle.net/10067/1658770151162165141>

1 Identification of ageing state clusters of reclaimed asphalt binders 2 using principal component analysis (PCA) and hierarchical cluster 3 analysis (HCA) based on chemo-rheological parameters

4 Alexandros Margaritis ^{a*}, Hilde Soenen ^b, Erik Fransen ^c, Georgios Pipintakos ^a,
5 Geert Jacobs ^a, Johan Blom ^a and Wim Van den bergh ^a

6 ^a *University of Antwerp, EMIB research group, Groenenborgerlaan 171, Antwerp 2020, Belgium*

7 ^b *Nynas NV, Groenenborgerlaan 171, Antwerp 2020, Belgium*

8 ^c *StatUa Center for Statistics, University of Antwerp, Venusstraat 35, Antwerp 2000, Belgium*

9 Abstract

10
11 Nowadays, Reclaimed Asphalt (RA) is widely used in pavement applications as part of new asphalt mixtures. To design high-
12 quality asphalt mixes, the RA material and especially the RA binder must be systematically characterised with the purpose to
13 explore its ageing state, especially when RA is added in high rates (above 20%). In this research, chemical (SARA and FTIR
14 ageing indexes) and rheological properties (master curve parameters, Glover-Rowe parameter and ΔT_c) of a large selection of
15 RA binders (19 samples) were determined to reveal their ageing level. The results of this experimental validation were further
16 analysed statistically to discover clusters of similar chemo-rheological properties, reflecting in this way their ageing state. The
17 exploratory techniques PCA and HCA were able to detect five clusters of RA binders with different ageing states. The five
18 clusters clearly distinguish the RA binders in groups with statistically different properties, assessed using one-way ANOVA.
19 The method proposed here is a potential tool to “fingerprint” RA binders with similar ageing states, particularly for decision-
20 making strategies, to optimise the use and treatment of RA.

21 Highlights:

- 22 • A large selection of RA binders was chemically and rheologically tested.
- 23 • Ageing states can be distinguished based on HCA and PCA analyses.
- 24 • RA binders showing similar basic properties differ in terms of their ageing state.

25 Keywords: reclaimed asphalt; asphalt binder ageing; clustering analysis; ageing states; bitumen relaxation;

26 1. Introduction

27 When a flexible pavement reaches its end-of-life point, the asphaltic layers can be milled and recycled in new
28 asphalt mixtures. The material derived from the milling process is labelled as Reclaimed Asphalt (RA). In the road
29 construction sector, RA induces considerable economic and ecological benefits [1, 2]. In order to ensure the high
30 performance of the mixture, essential steps must be considered for the comprehensive characterisation of the

31 components and most importantly, the RA material. Previous studies have demonstrated that adding RA can
32 strongly influence the mechanical properties, primarily when RA is utilised in higher percentages [3, 4].

33 In practice, RA is collected from different asphalt sources and layers with different original properties and
34 specifications. In Flanders, asphalt plants collect and classify the RA material according to the asphalt and
35 aggregate particle size distribution (“black” and “white” curve) and the penetration value of the recovered binder.
36 Based on those properties, RA is piled providing “homogeneous” RA material for future use, aiming to reduce
37 variability. The size of the site and the strategies for each asphalt plant can influence the number of piles and thus
38 create less or more homogeneously grouped material. The suitability of a RA binder is reflected by the penetration
39 value; according to the Flemish procurement regulations for road construction SB250 v3.1, RA binders with pen
40 lower of 10 are not permitted to be reused in new asphalt mixtures, since they are considered as extremely aged
41 [5]. Yet, penetration will not adequately capture other factors such as the crude oil source of bitumen, modification
42 presence and more importantly, its ageing history [6, 7].

43 When it comes to the performance characterisation, hitherto many researchers have investigated the changes in
44 physical, chemical and rheological properties that asphalt binders undergo during ageing. Bitumen chemistry can
45 unravel an undesirable effect called oxidative ageing of bitumen [8]. It is widely accepted that the severity of ageing
46 can be tracked by capturing the change in particular functional groups such as the sulfoxides and carbonyls [9-12].
47 From the newly formed compounds, carbonyls and carboxylic acids are of high polarity, having strong associations
48 with other active polar sites in the binder, as expressed through their Van der Waals forces. These polar compounds
49 of bitumen interact with each other, in some cases, reasonably strong [12]. This contributes towards increasing the
50 polar-polar interactions, leading eventually to an increment in viscosity. It is also accepted that an increase in
51 apparent molecular weight reduces the mobility of molecules to flow, which eventually will influence bitumen
52 rheology [10, 11, 13].

53 Moreover, bitumen can be characterised based on its solubility, which is affected by the size and polarity of
54 organic molecules, into four fractions: Saturates, Aromatics, Resins and Asphaltenes (SARA). The first three
55 fractions, i.e. Saturates, Aromatics and Resins, form a broader group, the Maltenes. In terms of bitumen ageing,
56 SARA classification allows for the quantification of the chemical changes in the bituminous binder, due to a
57 sequential reaction of aromatic to resin and finally to asphaltenes. Among these fractions, asphaltenes are
58 characterised by more polar molecular interactions, and they are considered as the principal responsible factor for
59 viscosity increase [8].

60 For the evaluation of the ageing process, specific criteria have been established to compare the extent of ageing
61 and predict to some extent, the related distresses. Previously, many studies have focused on the relationship
62 between oxidative ageing and alterations in physical properties of bitumen such as penetration, softening point,
63 viscosity, ductility and stiffness [14, 15]. In asphalt, the change of these properties can be related to adhesive and
64 cohesive bond strength with the mineral skeleton and lead eventually to cracking and ravelling. Bitumen is one of
65 the determining factors for asphalt pavement’s durability and long-life performance; therefore, high oxidative
66 ageing of asphalt binders leads to limited service life of the asphalt mixture. Ageing causes stiffening and brittleness
67 of the bitumen, translated by an increase of complex modulus (G^*) and a decrease of phase angle (δ) [14],
68 consequently leading to changes in the asphalt mixture performance, such as fatigue resistance [16].

69 Although major research focused on RA binders, has been confined to the determination of the aforementioned
70 physicochemical properties upon ageing, it still cannot reveal their ageing history without prior knowledge of the
71 properties during their original unaged state. Therefore, more extensive chemical and rheological characterisation
72 is essential to unravel information that can be linked to the extent of ageing of the asphalt binders. In this paper,
73 RA binders are evaluated and grouped according to their ageing severity, which from hereafter is defined as ageing
74 state, based on the chemical and rheological properties of the binder’s current condition.

75 A promising technique to approach the analysis of chemo-rheological properties is by using exploratory
76 statistical methods to detect patterns among the studied samples, based on similarities between the input data.
77 Among typical methods to detect such pattern structures are the Principal Component Analysis (PCA) and the
78 Hierarchical Cluster Analysis (HCA). This approach is well-reported and applied in other fields, namely in food

79 sciences [17, 18], in geochemistry studies [19] and physics [20]. In bitumen-related studies, Wang et al. have
80 successfully explored differences on asphalt binders manufacturers, using PCA on FTIR data [21]. In a similar
81 study, Ren et al. have classified asphalt binders derived from different crude oils using the same analytical approach
82 [22]. To the best of authors' knowledge, the abovementioned analyses have not been used previously to assess
83 differences in ageing of bituminous samples.

84 The objectives of this study are first to show the diversity in properties (chemical and rheological) between
85 different RA materials, secondly to assess the capability of penetration as a parameter to evaluate the ageing of the
86 RA binders and thirdly to classify the RA samples into clusters belonging into similar ageing states, on a chemo-
87 rheological basis.

88 2. Materials and methods

89 In total, 19 different RA binder samples have been collected for this research. Those samples were collected
90 from 4 different asphalt plants from the wider area of the Flemish region in Belgium:

- 91 • samples RA1 to RA7 collected from plant A
- 92 • samples RA8 to RA15, and RA18 collected from plant B
- 93 • samples RA16 and RA17 collected from plant C
- 94 • sample RA19 collected from plant D

95 For each RA binder sample, a sealed cup was collected with approximately 40 grams of extracted and recovered
96 binder. All samples were extracted and recovered by the asphalt plants (according to EN 12697-1:2012), as part of
97 their classification process, and delivered afterwards to our laboratory for further analyses. Two types of solvents
98 were used for the extraction, dichloromethane and trichloroethylene. The samples were first homogenised before
99 testing. We performed penetration (EN 1426:2015) and softening point (EN 1427:2015) tests on the samples, and
100 the results are presented in Figure 1. Three out of nineteen RA binders (samples RA8, RA11 and RA12), were
101 found to contain traces of SBS (Styrene-Butadiene-Styrene) modification. The procedure to determine the
102 modification presence is further explained in §2.3.

103 In the first stage of this research, all collected asphalt binders were subjected to a series of chemical and
104 rheological tests and then the experimentally defined data were further analysed by means of PCA and HCA. A
105 flowchart of the applied methodology is presented in Figure 2.

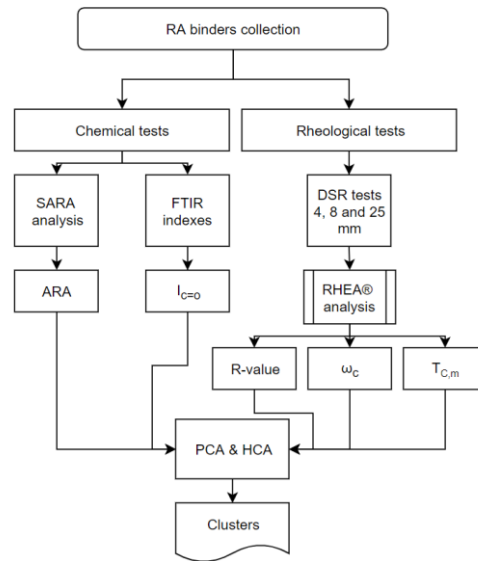
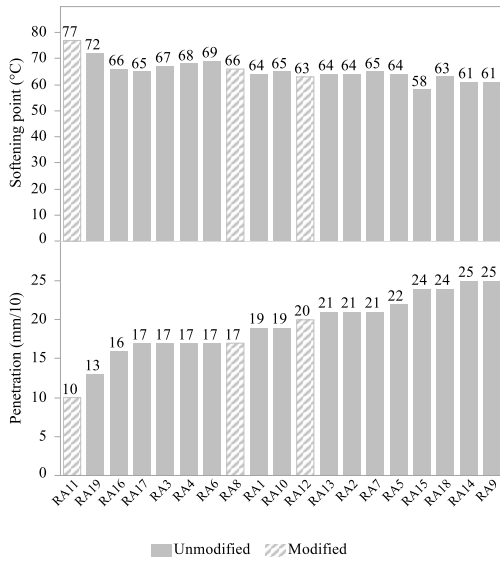


Figure 1: Penetration and softening point of the RA binders.

Figure 2: Flowchart of the applied methodology.

106

107 2.1. Rheological properties

108 To determine the rheological properties of the asphalt binders, frequency sweeps were conducted for a
 109 temperature range from -30 to $+70$ °C. The asphalt binders having SBS traces were tested till $+100$ °C to assess
 110 the activity of SBS modification further. Two devices were utilised to cover two temperature test ranges. From
 111 -30 till 0 °C (temperature increments of 6 °C), an Anton Paar™ MCR 101 was used to perform 4-mm tests, based
 112 on procedures described in [23, 24]. From 0 till 70 °C (temperature increments of 10 °C), an Anton Paar™ MCR
 113 500 was used for 8- and 25-mm tests, according to EN 14770:2012. The tests were performed under strain control,
 114 within the Linear Viscoelastic Region (LVR) of the samples, at a frequency sweep from 0.1 to 10 Hz. After
 115 performing strain sweeps to determine the LVR, it was found that for all samples a suitable, non-damaging, strain
 116 level was 0.02% for the 4-mm and 8-mm setup and 0.05% for the 25-mm geometry.

117 The DSR results were processed using the rheological software RHEA™, developed by Abatech Engineering
 118 Consultants [25]. The raw data are used as input for the software, and the software can generate the master curve.
 119 For the construction of the master curve, the Christensen-Andersen (CA) mathematical model was used on the
 120 shifted data [26, 27]. The software is using by default the Gordon and Shaw (G&S) shifting procedure [28]. The
 121 CA model describes the complex shear modulus (equation 1) in relation to the Glassy modulus (G_g), the rheological
 122 shape parameter (R) and the crossover frequency (ω_c) for every test frequency (ω). The shape parameter (R) can
 123 also be expressed as the difference between the log of glassy modulus and crossover modulus (where $G' = G'' = G_C$).
 124 All data, derived from -30 to $+70$ °C DSR tests, were shifted to a reference temperature $T_0 = 20$ °C. An example of
 125 a full master curve (based on 4-, 8- and 25-mm DSR tests) generated by the RHEA software is presented in Figure
 126 3. Due to binder amount limitations, one replicate was tested in 8- and 25-mm DSR tests and two replicates in
 127 4 mm DSR tests, for each RA binder sample.

128 Another promising rheological parameter is the Glover-Rowe (G-R) parameter, which is associated with fatigue
 129 cracking [29]. Rowe rearranged Glover's parameter, resulting in equation 2 [30]. The G-R parameter is calculated
 130 based on the measured G^* and δ at 15 °C and 0.005 rad/s. In this study, the G-R parameter was estimated from the

131 RHEA™ software based on the full CA master curves. Two limits have been proposed as damage thresholds: G-
 132 R = 150 kPa suggests cracking onset (warning) and G-R = 600 kPa suggests significant cracking (critical) [31].
 133 Increased G-R values indicate more brittle asphalt binders, susceptible to fatigue cracking, as demonstrated
 134 elsewhere [32, 33].

$$G^*(\omega) = G_g * \left[1 + \frac{\omega_c^{(\log 2/R)}}{\omega} \right]^{-R/\log 2} \quad 1$$

$$G - R = \frac{G^* * (\cos \delta)^2}{\sin \delta} \quad 2$$

135 The 4-mm DSR data were used to cover the high frequency-low temperature part of the master curve when
 136 approaching the glassy modulus. Another parameter estimated by the 4-mm DSR measurements was the low-
 137 temperature rheological parameters, more specifically the relaxation parameter m-value and the creep stiffness S(t).
 138 In previous studies, the use of 4-mm DSR tests has been demonstrated as an alternative of the Bending Beam
 139 Rheometer (BBR) test [34, 35]. The advantage of the former is that it requires a smaller bitumen amount: 25 mg
 140 instead of 15 gram per replicate.

141 ΔT_c is the difference between two lower continuous grading temperatures (equation 3), as proposed by ASTM
 142 D7643-16. When performing BBR tests, first the continuous grading temperature ($T_{c,s}$) is defined when
 143 $S(60) = 300$ MPa and then the continuous grading temperature ($T_{c,m}$) is defined when $m(60) = 0.300$. The parameter
 144 ΔT_c has been proposed by researchers as a parameter related to ageing induced cracking but also as an indicator of
 145 ageing evolution [36]. With ageing, ΔT_c becomes more negative, indicating deterioration of the asphalt binders
 146 performance, making them more susceptible to cracking. Two limits have been proposed in the past as performance
 147 indicators, the limit of $\Delta T_c = -2.5^\circ\text{C}$ as a warning limit and the limit $\Delta T_c = -5^\circ\text{C}$ as a critical limit [36]. Therefore
 148 ΔT_c is a useful parameter to track the performance of asphalt pavements but also characterise reclaimed asphalt
 149 binders before use. To estimate the ΔT_c parameter by DSR tests, the following conversion was applied, as proposed
 150 by MTE (Mathy Technology and Engineering) Services Inc. [34]:

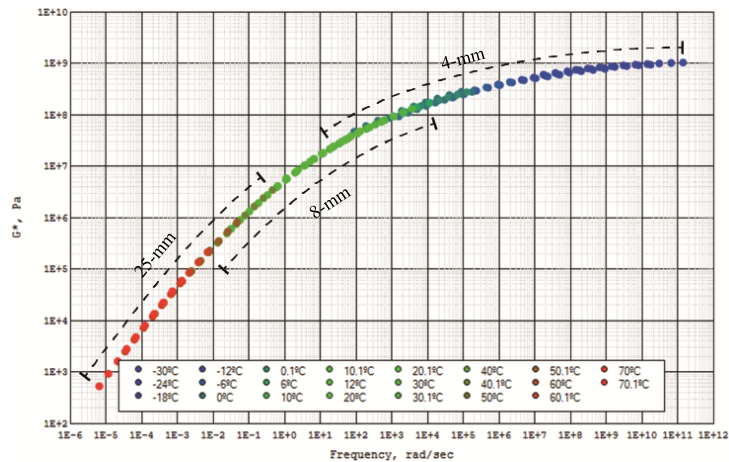
- 151 • $G(60) = 143$ MPa instead of $S(60) = 300$ MPa
- 152 • $m(60) = 0.275$ instead of $m(60) = 0.300$

153 The calculation of the new parameters ($T_{c,G}$ and $T_{c,m}$) follows the procedure proposed in ASTM D7643-16 based
 154 on the proposed conversions. Two relaxation moduli (G_1 and G_2) and two relaxation slopes (m_1 and m_2) at two
 155 temperatures (T_1 and T_2) must be determined, where $G_1 \leq 143 \text{ MPa} \leq G_2$ and $m_1 \leq 0.275 \leq m_2$. $T_{c,G}$ and $T_{c,m}$ are
 156 calculated based on equations 4 and 5.

$$\Delta T_c = T_{c,G} - T_{c,m} \quad 3$$

$$T_{c,G} = T_1 + \frac{(T_1 - T_2) * (\log 143 + \log G_1)}{\log G_1 - \log G_2} - 10 \quad 4$$

$$T_{c,m} = T_1 + \frac{(T_1 - T_2) * (0.275 + m_1)}{m_1 - m_2} - 10 \quad 5$$



158

159

Figure 3: Example of a master curve generated from RHEA software for a temperature range between - 30 and + 70 °C.

160 2.2. SARA fractioning

161 Several methods exist to determine the SARA fractions. Typical techniques are liquid chromatographic (LC)
 162 methods, such as the recently developed method by Sakib & Bhasin [37], and the Thin Layer Chromatography-
 163 Flame Ionization Detector (TLC-FID) method. In this study the TLC-FID method was applied, making use of a
 164 IATROSCAN MK-6s, according to the protocol described in IP 469/01 [38]. This protocol can be summarised in
 165 four steps. First, dilute, bitumen dichloromethane solutions 20mg/ml are prepared. Then, the solution is applied on
 166 a silica coated quartz rod; this step is also referred to as “spotting”. After spotting, the development of the sample,
 167 in different solvents takes place. For each bitumen sample, three rods were prepared. After the development of the
 168 fractions, the frame bearing 10 rods is inserted in the analyser, where the rods are sequentially passed through the
 169 flame ionisation detector (FID). A typical bitumen chromatogram consists of four peaks, where each peak
 170 represents one of the four generic fractions.

171 2.3. ATR-FTIR spectroscopy

172 Attenuated Total Reflectance Fourier Transform Infrared (ATR-FTIR) spectroscopy is an appropriate tool to
 173 trace oxidative ageing, and namely two functional groups: carbonyls and sulfoxides [39]. For the spectra
 174 acquisition, a Thermo Scientific Nicolet iS™ 10 FT-IR Spectrometer was utilised. Every spectrum was formed as
 175 the result of 32 repetitive scans and with a resolution of 4 cm⁻¹ in the range between 4000 cm⁻¹ and 400 cm⁻¹.

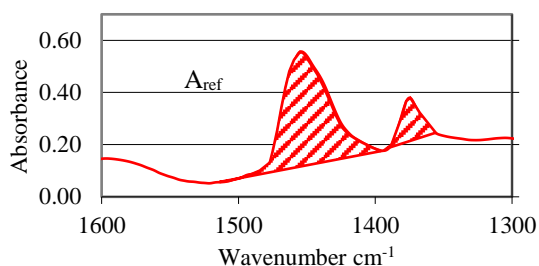
176 To qualitatively inspect the presence of modification, the BRRC protocol was applied [40]. Two types of
 177 modification are available in the Flemish market, Styrene-Butadiene-Styrene (SBS) and Ethylene-Vinyl-Acetate
 178 (EVA). These modifications, when present, show typical bands in the FTIR spectrum: at 700 and 968 cm⁻¹ for SBS
 179 and 1,240 and 1,740 cm⁻¹ for EVA.

180 To quantify the ageing indexes, the procedure described by Hofko et al. [41] was adopted. The selected protocol
 181 consists of two parts. First, the spectra are normalised and then the sulfoxide ($I_{S=O}$) and carbonyl ($I_{C=O}$) indexes are
 182 calculated. The applied normalisation consists of two steps. First, a baseline correction was applied, by shifting all
 183 spectra to zero absorbance at 1753 cm⁻¹. Second, an absorbance correction factor was applied, scaling all spectra
 184 to an absorbance of 1 at 2923 cm⁻¹. For the quantification of the ageing indexes, the applied baseline limits and
 185 equations are presented in Table 1.
 186

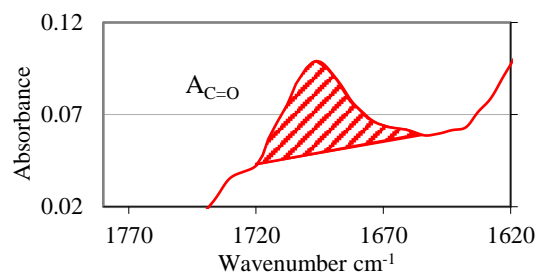
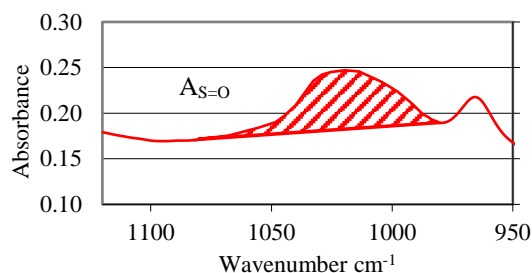
187

Table 1: Functional groups and their baseline limits used to calculate the ageing indexes.

Functional Group	Baseline Limits (cm ⁻¹)	Ageing Index
Aliphatic group (A _{ref})	1395-1350 1515-1395	A _{ref}
Carbonyl group (A _{C=O})	1720-1665	$I_{C=O} = \frac{A_{C=O}}{A_{ref}}$
Sulfoxide group (A _{S=O})	1082-980	$I_{S=O} = \frac{A_{S=O}}{A_{ref}}$



188



189

190

191

: Schematic illustration of the functional group spectra, attributed to the ageing indexes.

192

2.4. HCA and PCA analysis

193

HCA is a statistical tool that identifies clusters in the data, based on the similarities among the samples. The clustering of the samples is achieved by calculating the Euclidian distance between them, followed by stepwise clustering of the most similar variables. The result is typically depicted in a dendrogram, with shorter distances between the branches representing higher similarities between the samples. In this study, Ward's linkage criterion was selected. Both analyses were performed using the statistical software JMP® Pro 13.

198

199

200

201

202

203

204

205

206

PCA is an exploratory data analysis technique to represent the variation of the dataset, using a smaller number of linearly uncorrelated variables, referred to as principal components (PCs). Since the original variables may be on different measurement scales, original variables are typically centred and scaled. The standardised variables are then orthogonally transformed, so that the PCs are calculated as linear combinations of the original variables, whereby the first PC accounts for as much variance as possible, with the following PCs covering the largest possible variance that hasn't yet been covered by the preceding PCs. The number of PCs to retain is based upon how much of the variance is captured by the first PCs. Typically two PCs are retained in most cases, PC1 and PC2. In this study, the number of PCs was determined using the 80% variance criterion, meaning that the cumulative variance explained should be greater than 80%.

207 To detect ageing state patterns among the samples, a selection of the tested chemical and rheological parameters
 208 were selected as input variables for the PCA and HCA analyses. The selection criteria are based on two factors:
 209 firstly, the parameters should reflect the ageing evolution and secondly they should not be biased by other factors.

210 Various studies have reported the increase of asphaltenes and the simultaneous decrease of aromatics upon
 211 ageing. With regards to the saturates, most studies claim that they are unreactive through ageing, whereas resins
 212 can vary depending on the conditions and the crude oil [42]. Asphalt binders with lower ΔT_c suggest lower stress
 213 relaxation making them more prone to cracking, especially thermal cracking. With ageing, ΔT_c changes in an m-
 214 controlled mode [36, 43]. Therefore, to better reveal the differences between samples, the $T_{c,m}$ was incorporated in
 215 the analyses.

216 On the other hand, FTIR ageing indexes of RA binders can be biased, since part of the filler can remain after
 217 extraction and recovery. As a consequence this can have a big impact on the FTIR spectrum [44], especially in the
 218 case of calcareous filler which will give a signal at the approximately same band as the sulfoxide group [45],
 219 making it apparent that sulfoxide might not be an appropriate ageing indicator for RA binders. Furthermore,
 220 parameters such as the G-R parameter and $T_{c,G}$ can also indicate the ageing evolution but are also dependable to
 221 the stiffness of the virgin state of the material, which is not known. This can mislead the clustering results, since
 222 the ageing states will be driven by stiffness indicators, categorising the binders in the same, possibly false, approach
 223 that penetration does.

224 As a result, parameters that remain unreactive or less active throughout ageing, e.g. Saturates and $T_{c,G}$, or can be
 225 biased by other factors, e.g. $I_{S=O}$, were not included in the analyses. The remaining parameters were evaluated as
 226 appropriate since they can be related to the ageing history but also the source (supplier, crude oil, refining process,
 227 etc.) of the binder. Finally, the selected parameters to be incorporated in the analyses are the following:

- 228 • Chemical: Aromatics, Resins, Asphaltenes from SARA and $I_{C=O}$ from FTIR analysis.
- 229 • Rheological: shape parameter R, crossover frequency ω_c from CA model and the limiting critical
 230 temperature $T_{c,m}$, all associated with binder relaxation.

231 3. Results and discussion

232 The results of this paper are divided into two parts. The first part discusses the results of the experimental
 233 evaluation of all parameters tested for the RA binders while in the second part, the results of the pattern detection
 234 analyses are presented, using as initial variables the selected parameters described in section 2.4.

235 3.1. Experimental evaluation

236 3.1.1. Rheological properties

237 During ageing, it is generally accepted that the complex modulus G^* of asphalt binders increases, especially at
 238 the lower time-temperature domain of the master curve, while for the higher domain they reach a plateau at
 239 approximately 1 GPa [46], the so-called glass modulus G_g . To better capture, the differences between the samples,
 240 rheological parameters of the CA model were utilised, as presented in Figure 4. In this figure, the effect of ageing
 241 on the rheological parameters is demonstrated, showing an example of an unaged penetration grade bitumen 35/50
 242 and a RA binder. Comparing RA11 with the 35/50 bitumen, we observe a lower crossover frequency and modulus
 243 (ω_c and G_c), while the rheological index R increases. These observations are in line with findings in the literature
 244 [47, 48].

245 Figure 5 illustrates the master curves (experimental and fitted data) of four RA binders, RA8, RA11 and RA12
 246 that all contain traces of SBS modification and RA2, as an example of a non-modified binder. The CA model
 247 appears to fit well for both non-modified RA binders and RA binders with SBS traces. To further assess the activity

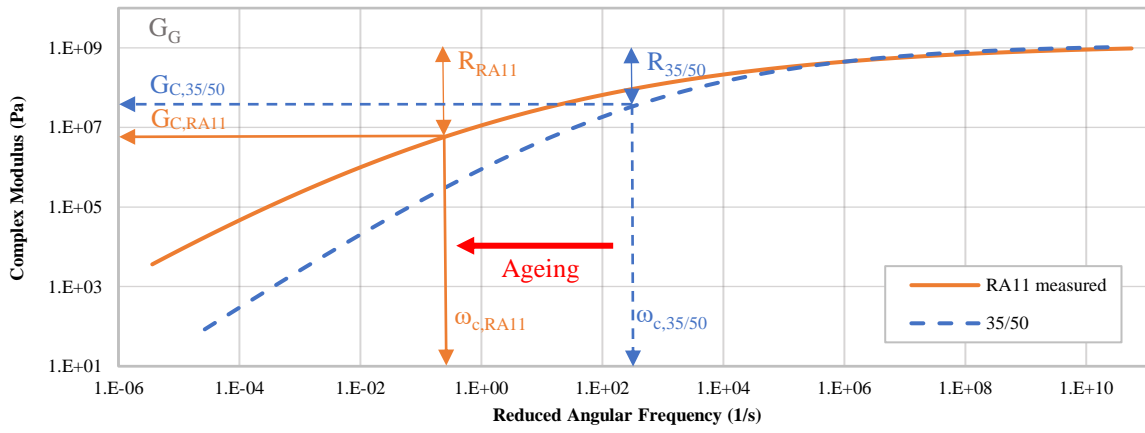
248 of SBS on the samples found to contain traces, the black curves of the same selection of RA binders (as in Figure
249 5) are presented in Figure 6. To be able to trace any possible increased elasticity at a higher temperature,
250 measurements were performed up to +100 °C. Comparing the RA binders with and without traces of SBS, only
251 sample RA11 shows a small increased elasticity compared to RA8 and RA12 and therefore higher polymer activity.
252 This observation might seem a contradictory result compared to the FTIR results that show modification presence,
253 but the almost non-modified behaviour of RA8 and RA12 can be attributed to the effects of field ageing or also to
254 a common practice applied by asphalt plants in Belgium. Typically, when asphaltic surface layers are milled, that
255 commonly contain PmB binders, are subsequently mixed with base layer RA material with unmodified bitumen.
256 The reasoning behind this practise is to avoid inserting RA material with high PmB content in the parallel drum
257 during reheating because this could lead to material sticking on the drum's wall and with an increased risk of
258 creating RA agglomerations, leading eventually to clogging.

259 The evolution of ageing can also be visualised by plotting ω_c vs R, where ageing is directed by a simultaneous
260 increase of R and decrease of ω_c , as presented in Figure 7a [49, 50]. Figure 7b shows the space diagram ω_c vs R of
261 the RA binders. Comparing Figure 7a and 8b, the same trend can be detected: a movement to the bottom right
262 corner during different ageing simulations and different samples accordingly. It is evident, based on these figures,
263 that the RA binders demonstrate different rheological responses attributed mainly to their ageing.

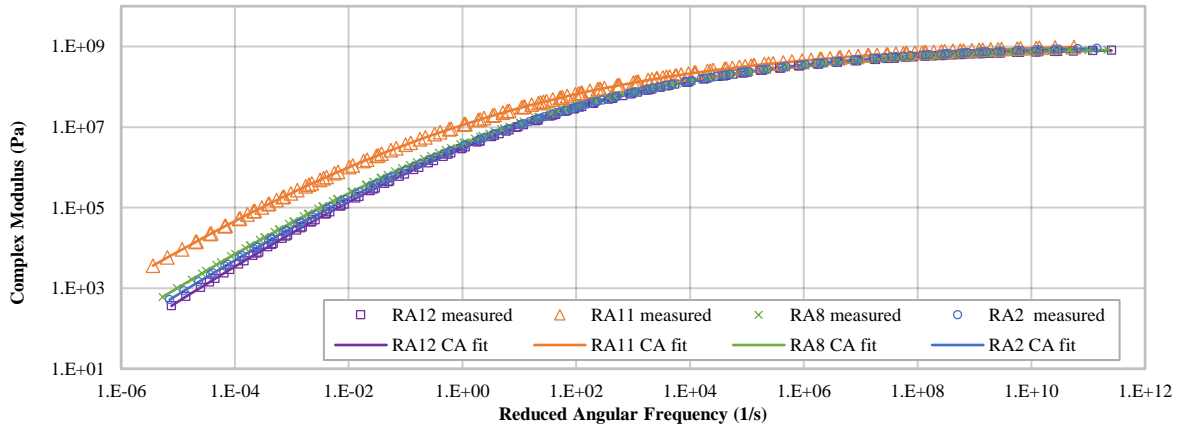
264 The G-R parameter results are illustrated in black space representation in Figure 8. Sample RA11 is positioned
265 above the critical limit, while samples RA6, RA19, RA4 and RA16 are placed within the damage thresholds. It is
266 expected that under consecutive ageing step simulations, a movement to the top left corner of the black space
267 diagram will be observed, meaning that with ageing a simultaneous increase of G^* with a decrease of δ is expected.
268 The fact that the sample RA11 exhibits the highest G^* and lowest δ might mean that this binder is more aged
269 compared to the rest; however, this result can be strongly influenced also by the fact that RA11 show SBS
270 modification traces. Practically the presence of the SBS modification will alter the rheological response of the
271 material in high temperature-low frequency (0.005 rad/s) domains, leading to higher G^* and lower δ compared to
272 neat bitumen [51]. Therefore, the G-R parameter might be overestimated for the case of polymer modified binders.
273 Another observation is that the RA binders follow the same trend ($R^2=0.8994$), as depicted by the fitted trend-line
274 of G-R data (Figure 8). This surprising trend could be explained as if the binders "age" at the same rate. Petersen
275 observed the same conclusion for the SHRP asphalt binders in 2009, where he supported that climate conditions
276 influence greatly the oxidative ageing [8]. The last point supports the observation above since all the RA binders
277 were collected from the same part of the country, where very similar climate conditions exist.

278 Together with the rheological parameters, the ΔT_c parameter was also determined. The ΔT_c results of the RA
279 binders (see Figure 9) show a different trend compared to the rheological parameters. Samples RA9, RA14 and
280 RA15 exhibit high ΔT_c indicating less aged samples, which is in agreement with the conclusion of the rheological
281 parameters ω_c and R. However, RA binders with the lowest penetration value, that would be conventionally
282 characterised as the most aged ones, do not exhibit the lowest ΔT_c while it is also demonstrated that ageing leads
283 to lower ΔT_c . A possible explanation here might be the starting point (unaged state) and the service years of the
284 binder samples, where RA11 (10 mm/10) could have been a stiffer binder compared to RA8 (17 mm/10 & highest
285 ΔT_c) during their virgin state and/or the former was for a shorter period of time in service compared to the latter.

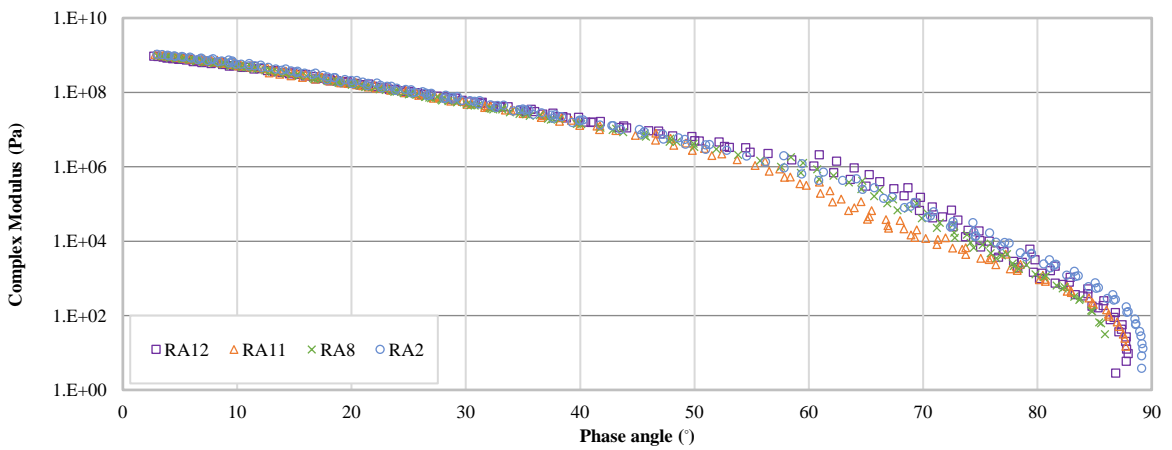
286 One should note here that only the master curve and the rheological parameters, cannot independently reveal
287 the ageing state. A direct conclusion concerning their ageing state could effectively be drawn only in the case that
288 all the RA binders have the same starting point, meaning similar properties in their virgin state. This highlights the
289 necessity to consider both rheological and chemical indicators to reflect the current ageing state better.



290
291 Figure 4: Evolution of rheological parameters (ω_c , R and G_c) with ageing; an example of unaged bitumen (35/50 pen grade) and RA binder.

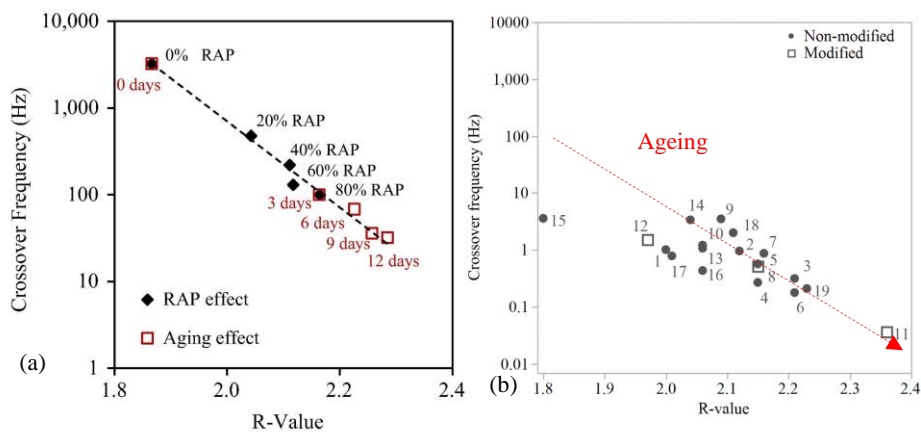


292
293 Figure 5: CA master curve of RA binders found to contain SBS traces (RA8, RA11 and RA12) and of one non-modified RA binder (RA2).



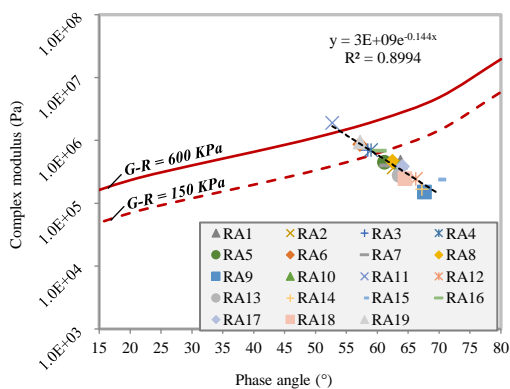
295
296 Figure 6: Black curve diagrams of RA binders found to contain SBS traces (RA8, RA11 and RA12) and of one non-modified RA binder (RA2).

298



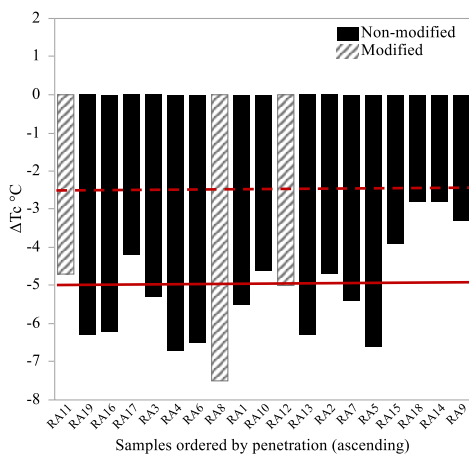
299

300 Figure 7: Effect of ageing on the evolution of ω_c vs R, based on literature [50] (a), the evolution of ω_c vs R for the different RA binders (b).



301

302 Figure 8: Representation of the G^* and δ of the G-R parameter in black space diagram, for the various RA binders.



303

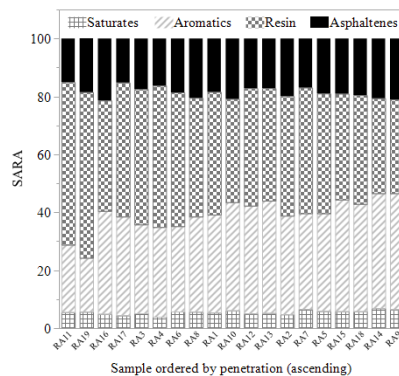
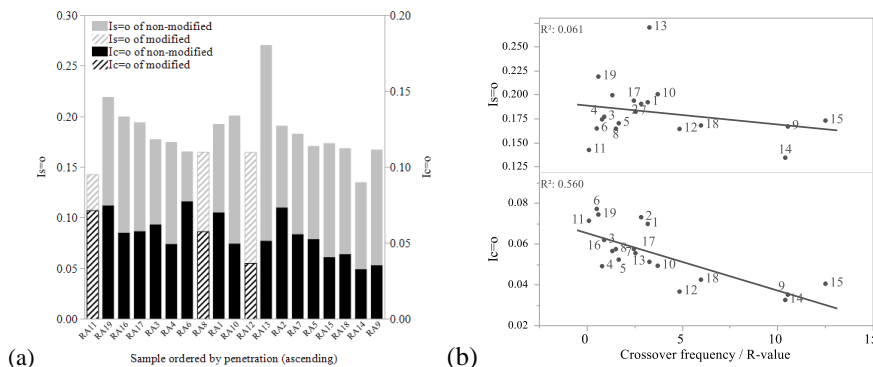
304 Figure 9: ΔT_c parameter of the RA binders

305 3.1.2. Chemical properties

306
 307 The RA binders were chemically evaluated in terms of SARA fractionation, carbonyl and sulfoxide indexes.
 308 The SARA fractions were quantified using the TLC-FID method. Figure 10 presents the results of the RA samples.
 309 The first observation is that among all samples, saturates remain stable ($5.55 \% \pm 0.73 \%$), which corresponds to
 310 the view that saturates remain inactive during ageing [42]. The rest of the fractions show a considerable variation
 311 among the samples showing the following trend: stiffer binders show lower aromatics and higher resins, which can
 312 be attributed to the expected transformation of aromatics to resins upon oxidation. The asphaltenes do not show
 313 any distinguishable trend. The differences between the SARA fractions could also be credited to different binder
 314 sources, derived from different crude oils and/or under different refining processes.

315 An additional tool that has been proved able to trace ageing is the evolution of certain functional groups using
 316 FTIR spectroscopy, namely carbonyl and sulfoxide groups. In Figure 11a, the results of $I_{C=O}$ and $I_{S=O}$ indexes are
 317 presented. Samples RA6, 11 and 19 show the highest $I_{C=O}$ values, where samples RA13 and 19 the highest $I_{S=O}$. As
 318 can be seen from Figure 11b, a trend can be observed ($R^2 = 0.560$) between $I_{C=O}$ and the rheological parameters of
 319 the master curve.

320 On the other hand, $I_{S=O}$ seems to be uncorrelated ($R^2 = 0.061$) for this set of data. There is widespread empirical
 321 evidence that carbonyls have shown a good correlation with the viscosity increase during long-term oxidation in
 322 contrary to sulfoxides that appeared to demonstrate weak correlation [52, 53]. A possible explanation of this weak
 323 association can be attributed to the presence of calcareous filler leftovers after the extraction and recovery process,
 324 biasing the band quantification at 1030cm^{-1} , which is the same for the sulfoxides and the filler [45].
 325

326
327 Figure 10: SARA fractions of RA binders328
329 Figure 11: Carbonyl and Sulfoxide index of RA binders (a), correlation of Carbonyl and Sulfoxide index against the ratio of Crossover
330 frequency over R-value (combined effect)

331 3.2. Pattern detection analysis

332 To visualise subgroups in the data and to detect ageing state patterns based on chemo-rheological similarities,
 333 two exploratory multivariate data analysis techniques were applied, including Principal Component Analysis
 334 (PCA) and Hierarchical Cluster Analysis (HCA).

335 HCA calculates the multidimensional Euclidian distances, between the observations, starting from the initial
 336 variables. In this study, as input variables were considered only the selected parameters, described in the methods
 337 section (§2.4). Using a stepwise algorithm (Ward's linkage criterion), observations behaving similarly across the
 338 initial variables are linked, and the results are graphically shown in a clustering tree (dendrogram). To determine
 339 the clusters, groups of observations behaving similarly, a cut-off point must be selected.

340 Based on visual inspection of the derived dendrogram and the selected cut-off point (see Figure 12), the RA
 341 samples can cluster in 5 subgroups:

- 342 • Cluster 1: samples RA9, 14 and 15
- 343 • Cluster 2: samples RA10,12,13 and 18
- 344 • Cluster 3: samples RA1, 2, 5, 6, 8 and 16
- 345 • Cluster 4: samples RA3, 7, 4 and 17
- 346 • Cluster 5: samples RA11 and 19

347 PCA starts from the correlation between the initial variables (selection of parameters presented in §2.4), and
 348 represents the variation of the dataset, using a reduced number of linearly uncorrelated variables, referred to as
 349 principal components (PCs) [54]. PCs are calculated as linear combinations of the original variables. Table 2
 350 contains the coefficients (the "loadings") through which the PCs are calculated based upon the initial variables.
 351 Observations with a strongly positive PC1 value have high values of Resin, $T_{c,m}$, $I_{C=O}$ and R, and low values of ω_c
 352 and aromatics. Whereas a sample with a strongly positive value for PC2 will have a high value for asphaltenes.
 353 The PCs are constructed in such a way that the first PC, i.e. PC1, accounts for as much variance as possible, with
 354 the following PCs covering the largest possible variance that hasn't yet been covered by the preceding PCs.

355 In the current dataset, PC1 explains 70.5 % and PC2 12.5 % of the total variance of the dataset, with the
 356 cumulative variance explained by PC1 and PC2 reaching 83 %, meeting the 80% variance criterion. Figure 13a
 357 represents the plot of the PC1 score versus the PC2 score, which illustrates the position of the samples in a new
 358 coordinate system formed by PC1 and PC2. In Figure 13b each arrow represents an original variable, and the
 359 correlation between two original variables is proportional to the cosine of the angle between them. Table 2 presents
 360 the factor loadings of both PCs. More specifically, PC1 is positively correlated with Resin, $I_{C=O}$, R and $T_{c,m}$ while
 361 negatively correlated with aromatics and ω_c . PC2 is negatively correlated only with Asphaltenes.

362 Based on the score plot we can conclude that the clusters 1, 2 and 3 are driven by PC1, cluster 1 and 2 in the
 363 low positive side of PC1 and cluster 3 in the high positive, where high values for Resins, $I_{C=O}$, R and $T_{c,m}$ result in
 364 a strongly positive value of PC1. On the other hand, cluster 4 and 5 are characterised by negative PC1 values, which
 365 is driven by high values of aromatics and ω_c , which have negative loadings on PC1. PC1 explains the more
 366 substantial part of the data variance (70.5 %) showing high loadings for most of the inserted factors (except the
 367 asphaltenes). In line with this observation, 4 out of 5 clusters can be distinguished based on PC1.

368 Although the HCA dendrogram suggests that cluster 1 and 2, as well as cluster 4 and 5 could be merged if a
 369 higher cut-off would be selected, the PCA score plot shows a clear distinction between the 4 clusters. Cluster 1 and
 370 2 are separated mainly by their PC2 score. Since asphaltenes show a strong loading on PC2, this implies that cluster
 371 1 and 2 differ in asphaltenes, whereas clusters 4 and 5 differ by their PC1 score, which is driven by high aromatics
 372 and ω_c . This observation enables a better interpretation of the results and the underlying structure of the clusters.

373 Using one-way ANOVA (Analysis of Variance), we determined which of the original parameters incorporated
 374 in the HCA and PCA analysis differ between the clusters. Across all parameters inserted in the PCA and HCA, we
 375 observe a significantly different mean value between the clusters (p-value < 0.05). Mean values for each parameter
 376 within the 5 clusters are illustrated in Figure 14.

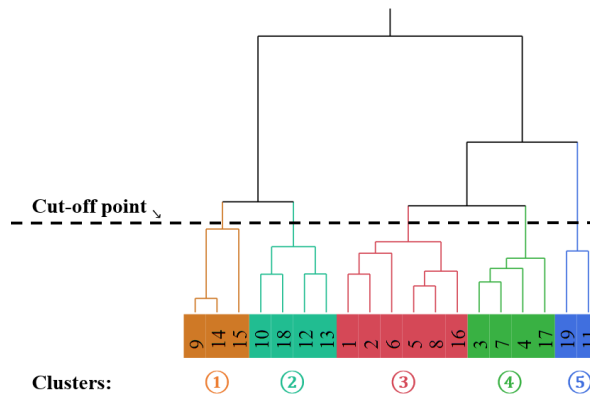
377 Cluster 1 and 2 (red and green) have similar rheological parameters (Figure 14 a, e, f and g) but belong to
 378 different asphaltenes class (Figure 14 c). It appears that from a rheological point of view, the samples belong to

379 similar ageing states but not based on their asphaltenes, while it is known that asphaltenes increase during ageing.
 380 An assumption could be that the starting point of asphaltenes was different, but their evolution might have been
 381 similar. This assumption can lead us to the conclusion that those clusters might belong to a different supplier and/or
 382 different crude oil since SARA fractions strongly relate to the binder source. Therefore, PC2 may exhibit
 383 differences in the asphalt binder source. Cluster 3 shows the highest PC1 values and as it can be seen by the mean
 384 values of Figure 14, the highest values in Resin, R, $T_{c,m}$, $I_{C=O}$, which indicates the most aged samples. On the
 385 contrary, Cluster 4 shows the lowest PC1 value, thus the less aged group of binders with the highest ω_c and the
 386 lowest $I_{C=O}$. Consequently, it is evident that PC1 can illustrate the ageing state.

387 The results of the clustering analysis demonstrate also the inability of conventional properties (penetration,
 388 softening point and penetration index) to distinguish between the ageing state of RA binders and as a consequence
 389 to comprehensively characterise the RA binder.

390 Figure 15 shows the mean values of the three commonly used conventional properties among the defined
 391 clusters. Clusters 1 and 5 are in accordance with the high and low penetration groups. On the contrary, the
 392 intermediate penetration groups show no differentiation while the ageing state clusters do. The same observations
 393 apply also for softening point and the penetration index. The main reason behind this trend is that the conventional
 394 properties are able to roughly express the mechanical response of the material at intermediate and high temperature
 395 as the DSR does, but the ageing states are also based on chemical parameters ($I_{C=O}$ and part of SARA parameters),
 396 data that cannot be reflected by the conventional properties.

397 The result of the clustering analysis, based on PCA and HCA techniques, proved to be a very useful tool. As
 398 clearly illustrated, it offers the ability to explore and then define RA binder clusters based upon chemical and
 399 rheological properties that alter with ageing. Additionally, the clustering method can be further implemented as
 400 part of a decision-making tool. Such a tool can be used for various purposes. First, it could verify the suitability of
 401 certain RA materials for specific RA percentage range, for example lower or higher percentage depending on the
 402 ageing state cluster; second, it could verify the use of RA for certain pavement layers, for example less aged RA
 403 clusters could be used as part of surface asphalt layers, moderately aged clusters in base asphalt layers and highly
 404 in unbound base layer; lastly it could depict the need or not of certain additives, such as the use of rejuvenators for
 405 the more aged clusters.
 406



407

408

Figure 12: Dendrogram of HCA on the RA binders, based on selected variables; the cut-off point discriminates the five clusters.

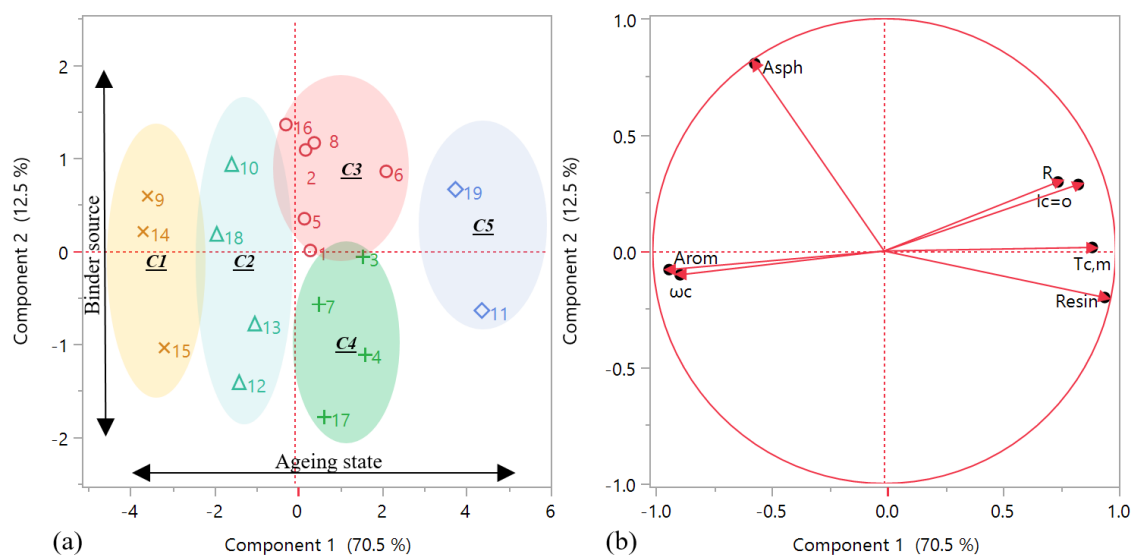


Figure 13: PCA score plot of the RA samples (a) and loading plot of the parameters based on PC1 and PC2 (b)

409

410

411

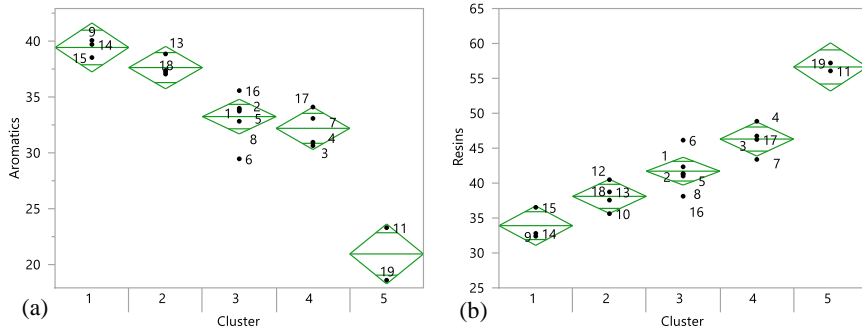
Table 2: Loading matrix of PC1 and PC2

Variable	PC1	PC2
Resin	0.953	-0.200
T _{c,m}	0.899	0.015
I _{C=O}	0.839	0.286
R	0.751	0.297
Asphaltenes	-0.559	0.806
ω _c	-0.881	-0.102
Aromatics	-0.929	-0.080

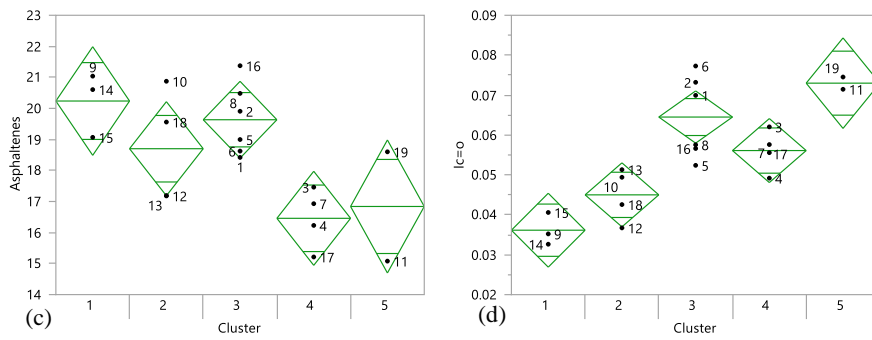
In bold loading factors >0.60

412

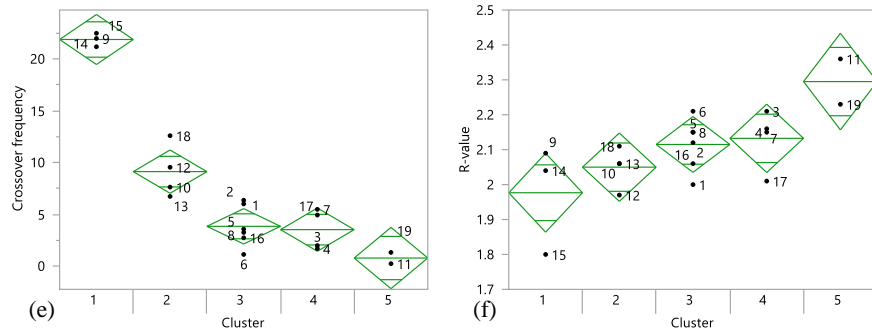
413



414



415



416

417

418

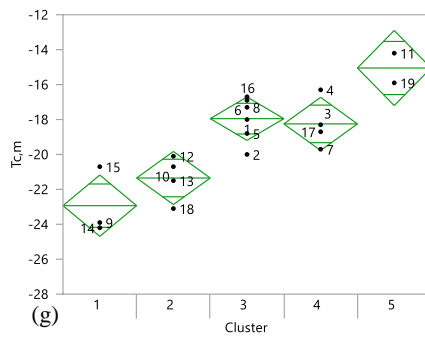


Figure 14: Mean value plots of the parameters inserted in the analyses against the defined clusters, a) aromatics, b) resins, c) asphaltenes, d) I_{C=O}, e) ω_C, f) R and g) ΔT_C.

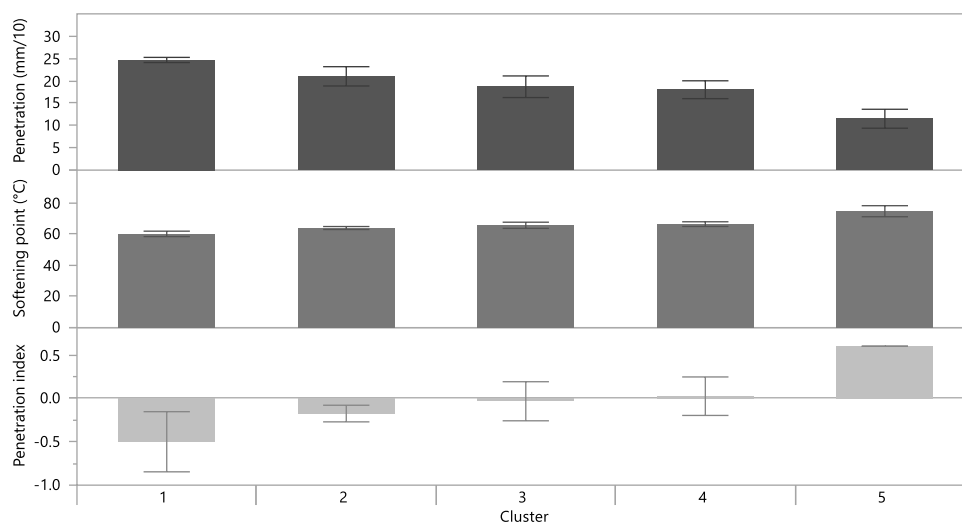


Figure 15: Mean values of conventional parameters (penetration, softening point and penetration index) for the defined clusters.

419

420

421 4. Conclusions

422 In this study, a set of different RA binders was evaluated, chemically and rheologically, and then statistically
 423 analysed using HCA and PCA techniques to detect patterns among them based on properties' similarities. Based
 424 on the experimental evaluation of 19 randomly collected RA binders, the following conclusions can be drawn:

- 425 • Rheological parameters showed differences in ageing of the RA binders, as also demonstrated in other
 426 studies. More aged asphalt binders showed a simultaneous increase of R and a decrease of ω_c .
- 427 • RA binders found to contain SBS traces exhibited almost similar or lower elasticity at higher temperatures,
 428 when tested using DSR, compared to non-modified RA binders.
- 429 • ΔT_c and $I_{C=O}$ did not demonstrate the same trend as the rheological properties, especially in the
 430 intermediate penetration group binders (15-20 mm/10). A possible explanation could be related to
 431 differences in the virgin binders, or to the different aging conditions the virgin materials were exposed to,
 432 and also to variations in the layer depth or the layer type they originate from.
- 433 • Conventional properties, such as penetration, softening point and penetration index, are less accurate
 434 compared to using a combination of chemical and rheological parameters to characterise the RA binders.
 435 Furthermore, conventional properties fail to demonstrate properties associated with distress phenomena
 436 such as G-R and ΔT_c , derived by DSR tests. Those properties are particularly important when it comes to
 437 ageing assessment.

438 Based on the HCA and PCA analyses:

- 439 • It has been demonstrated that pattern detection techniques (in this case HCA and PCA) can be utilised to
 440 detect clusters of asphalt binders with similar properties, reflecting this way the ageing state of each
 441 cluster.
- 442 • The variables inserted in the analyses, are reliable indicators that individually can provide insight about
 443 the ageing severity. The advantage of incorporating them in the HCA and PCA analyses is the
 444 demonstration of a combined chemo-rheological effect on the ageing states.
- 445 • Binders with the same penetration can belong to different clusters, indicating different ageing states.

- 446 • Clusters might also exhibit the source of the binder. This statement could have been more in-depth
 447 explored if more information concerning the element composition were analysed, such as nickel and
 448 vanadium content, but it was not in the scope of this research.
 449 • The generic SARA fractions provided information concerning ageing but also information that can be
 450 attributed to the binder source, as illustrated by the PCA.

451 This study highlights the necessity of considering more advanced parameters (compared to the current
 452 conventional properties) and pattern detection techniques, for the comprehensive characterisation of the ageing
 453 state of RA materials. This approach is especially important for the optimisation of new mixtures with high
 454 recycling rates. The presented method is capable of distinguishing ageing states that can be further exploited to
 455 make decisions concerning the selection of RA materials for certain applications (e.g. certain pavement layers), to
 456 decide recycling rate thresholds or for the selection of additives (e.g. use of rejuvenators).

457 **Acknowledgements**

458 The authors would like to acknowledge the University of Antwerp for the Doctoral funding, as well as Willemen
 459 Infra (former Van Wellen and Aswebo), TopAsfalt and Belasco for providing the RA binder samples. Also, Mats
 460 Andersson and Xiaohu Lu from Nynas AB for providing the infrastructure (equipment and guidance) for the SARA
 461 fractionation.

462 **Disclosure statement**

463 No potential conflict of interest was reported by the authors.

464 **References**

- 465 1. Mantalovas, K. and G. Di Mino, *The Sustainability of Reclaimed Asphalt as a Resource for Road*
 466 *Pavement Management through a Circular Economic Model*. 2019. **11**(8): p. 2234.
 467 2. Anthonissen, J., W. Van den bergh, and J. Braet, *Review and environmental impact assessment of green*
 468 *technologies for base courses in bituminous pavements*. Environmental Impact Assessment Review, 2016.
 469 **60**: p. 139-147.
 470 3. Al-Qadi, I.L., et al., *Impact of high RAP contents on structural and performance properties of asphalt*
 471 *mixtures*. 2012.
 472 4. Margaritis, A., J. Blom, and W. Van den bergh, *Evaluating the mechanical performance of Flemish*
 473 *bituminous mixtures containing RA by statistical analysis*. Road Materials and Pavement Design, 2019:
 474 p. 1-15.
 475 5. Agentschap Wegen en Verkeer, *Standaardbestek 250 voor de wegenbouw - versie 3.1*. 2014.
 476 6. Jones, D.R., *SHRP materials reference library: Asphalt cements: A concise data compilation*. Vol. 1.
 477 1993: Strategic Highway Research Program, National Research Council Washington, DC.
 478 7. Nicholls, C., *BitVal: Analysis of Available Data for Validation of Bitumen Tests*. 2006: Report on Phase
 479 1 of the BiTVAl Project.
 480 8. Petersen, J.C., *A review of the fundamentals of asphalt oxidation: chemical, physicochemical, physical*
 481 *property, and durability relationships*. Transportation Research Circular, 2009(E-C140).
 482 9. Petersen, J.C. and P.M. Harnsberger, *Asphalt aging: dual oxidation mechanism and its interrelationships*
 483 *with asphalt composition and oxidative age hardening*. Transportation Research Record, 1998. **1638**(1):
 484 p. 47-55.

- 485 10. Dony, A., et al. *MURE National Project: FTIR spectroscopy study to assess ageing of asphalt mixtures*.
486 in *Proceedings of the E&E congress*. 2016.
- 487 11. Tauste, R., et al., *Understanding the bitumen ageing phenomenon: A review*. Construction and Building
488 Materials, 2018. **192**: p. 593-609.
- 489 12. Branthaver, J.F. and S.C. Huang, 2 - *Analytical separation methods in asphalt research*, in *Advances in*
490 *Asphalt Materials*, S.-C. Huang and H. Di Benedetto, Editors. 2015, Woodhead Publishing: Oxford. p.
491 31-57.
- 492 13. Lu, X. and U. Isacson, *Effect of ageing on bitumen chemistry and rheology*. Construction and Building
493 Materials, 2002. **16**(1): p. 15-22.
- 494 14. Molenaar, A.A.A., E.T. Hagos, and M.F.C. van de Ven, *Effects of Aging on the Mechanical*
495 *Characteristics of Bituminous Binders in PAC*. Journal of Materials in Civil Engineering, 2010. **22**(8): p.
496 779-787.
- 497 15. Weigel, S. and D. Stephan, *Modelling of rheological and ageing properties of bitumen based on its*
498 *chemical structure*. Materials and Structures, 2016. **50**(1): p. 83.
- 499 16. Kim, Y.R., et al., *Long-term aging of asphalt mixtures for performance testing and prediction*. 2018:
500 Transportation Research Board.
- 501 17. Yi, T., et al., *Comparison of ten major constituents in seven types of processed tea using HPLC-DAD-MS*
502 *followed by principal component and hierarchical cluster analysis*. LWT - Food Science and Technology,
503 2015. **62**(1, Part 1): p. 194-201.
- 504 18. Patras, A., et al., *Application of principal component and hierarchical cluster analysis to classify fruits*
505 *and vegetables commonly consumed in Ireland based on in vitro antioxidant activity*. Journal of Food
506 Composition and Analysis, 2011. **24**(2): p. 250-256.
- 507 19. Jiang, Y., et al., *Principal component analysis and hierarchical cluster analyses of arsenic groundwater*
508 *geochemistry in the Hetao basin, Inner Mongolia*. Geochemistry, 2015. **75**(2): p. 197-205.
- 509 20. Robledo, J.I., et al., *Exploratory Methodology for Retrieving Oxidation State Information from X-ray*
510 *Resonant Raman Scattering Spectrometry*. Analytical Chemistry, 2015. **87**(7): p. 3639-3645.
- 511 21. Wang, K., et al., *Application of attenuated total reflectance Fourier transform infrared (ATR-FTIR) and*
512 *principal component analysis (PCA) for quick identifying of the bitumen produced by different*
513 *manufacturers*. Road Materials and Pavement Design, 2018. **19**(8): p. 1940-1949.
- 514 22. Ren, R., et al., *Identification of asphalt fingerprints based on ATR-FTIR spectroscopy and principal*
515 *component-linear discriminant analysis*. Construction and Building Materials, 2019. **198**: p. 662-668.
- 516 23. Gražulytė, J., et al., *Analysis of 4-mm DSR tests: calibration, sample preparation, and evaluation of*
517 *repeatability and reproducibility*. Road Materials and Pavement Design, 2019: p. 1-15.
- 518 24. TechBrief., F.H.A., *Four-mm Dynamic Shear Rheometry*. 2017, FHWA, US Department of
519 Transportation Washington, DC: Washington, D.C.
- 520 25. Abatech, *Rheology Analysis Software, version 2.3, Abatech*. 2011: Blooming Glen, PA.
- 521 26. Christensen Jr, D.W. and D.A. Anderson. *Interpretation of dynamic mechanical test data for paving grade*
522 *asphalt*. in *Asphalt Paving Technology: Association of Asphalt Paving Technologists-Proceedings of the*
523 *Technical Sessions*. 1992.
- 524 27. Anderson, D.A., et al., *Binder characterization and evaluation, volume 3: Physical characterization*.
525 1994.
- 526 28. Gordon, G. and M. Shaw, *Computer Programs for Rheologists*. 1994, New York: Hanser.
- 527 29. Glover, C.J., et al., *Development of a new method for assessing asphalt binder durability with field*
528 *validation*. 2005, Texas Dept Transport. p. 1-334.
- 529 30. Rowe, G., G. King, and M. Anderson, *The influence of binder rheology on the cracking of asphalt mixes*
530 *in airport and highway projects*. Journal of Testing Evaluation, 2014. **42**(5): p. 1063-1072.
- 531 31. Rowe, G., *Prepared discussion for the AAPT paper by Anderson et al.: Evaluation of the relationship*
532 *between asphalt binder properties and non-load related cracking*. Journal of the Association of Asphalt
533 Paving Technologists, 2011. **80**: p. 649-662.

- 534 32. Elkashef, M., et al., *Preliminary examination of soybean oil derived material as a potential rejuvenator*
535 *through Superpave criteria and asphalt bitumen rheology*. Construction and Building Materials, 2017.
536 **149**: p. 826-836.
- 537 33. Hao, G., et al., *Effect of aging on chemical and rheological properties of SBS modified asphalt with*
538 *different compositions*. Construction and Building Materials, 2017. **156**: p. 902-910.
- 539 34. Christensen, D., et al., *Past, Present, and Future of Asphalt Binder Rheological Parameters: Synopsis of*
540 *2017 Technical Session 307 at the 96th Annual Meeting of the Transportation Research Board*. 2019,
541 Transportation Research Circular.
- 542 35. Sui, C., et al., *New Low-Temperature Performance-Grading Method: Using 4-mm Parallel Plates on a*
543 *Dynamic Shear Rheometer*. Transportation Research Record, 2011. **2207**(1): p. 43-48.
- 544 36. Anderson, R.M., et al., *Evaluation of the relationship between asphalt binder properties and non-load*
545 *related cracking*. Journal of the Association of Asphalt Paving Technologists, 2011. **80**.
- 546 37. Sakib, N. and A. Bhasin, *Measuring polarity-based distributions (SARA) of bitumen using simplified*
547 *chromatographic techniques*. International Journal of Pavement Engineering, 2019. **20**(12): p. 1371-1384.
- 548 38. Energy Institute, *IP 469/01: Determination of saturated, aromatic and polar compounds in petroleum*
549 *products by thin layer chromatography and flame ionization detection*. 2006.
- 550 39. Marsac, P., et al., *Potential and limits of FTIR methods for reclaimed asphalt characterisation*. Mater
551 Struct, 2014. **47**(8): p. 1273-1286.
- 552 40. Piérard, N., *Bitumen analysis with FTIR spectrometry: processing of FTIR spectra*. 2013, BRRC:
553 Brussels.
- 554 41. Hofko, B., et al., *Repeatability and sensitivity of FTIR ATR spectral analysis methods for bituminous*
555 *binders*. Mater Struct, 2017. **50**(3): p. 187.
- 556 42. Lu, X. and U. Isacson, *Artificial aging of polymer modified bitumens*. Journal of Applied Polymer
557 Science, 2000. **76**(12): p. 1811-1824.
- 558 43. Cao, W., et al., *Chemical and rheological evaluation of asphalts incorporating RAP/RAS binders and*
559 *warm-mix technologies in relation to crack resistance*. Construction and Building Materials, 2019. **198**:
560 p. 256-268.
- 561 44. Makowska, M. and T. Pellinen. *The “false positive” on the antiaging properties of asphalt fines*
562 *investigated by RTFO laboratory aging of mastics*. in *Functional Pavement Design: Proceedings of the*
563 *4th Chinese-European Workshop on Functional Pavement Design (4th CEW 2016, Delft, The*
564 *Netherlands, 29 June-1 July 2016)*. 2016. CRC Press.
- 565 45. Margaritis, A., et al., *On the Applicability of ATR-FTIR Microscopy to Evaluate the Blending between*
566 *Neat Bitumen and Bituminous Coating of Reclaimed Asphalt*. Coatings, 2019. **9**(4).
- 567 46. Qin, Q., et al., *Field aging effect on chemistry and rheology of asphalt binders and rheological predictions*
568 *for field aging*. Fuel, 2014. **121**: p. 86-94.
- 569 47. Grilli, A., M.I. Gnisci, and M. Bocci, *Effect of ageing process on bitumen and rejuvenated bitumen*.
570 Construction and Building Materials, 2017. **136**: p. 474-481.
- 571 48. Christensen, D.W., D.A. Anderson, and G.M. Rowe, *Relaxation spectra of asphalt binders and the*
572 *Christensen–Anderson rheological model*. Road Materials and Pavement Design, 2017. **18**(sup1): p. 382-
573 403.
- 574 49. Mogawer, W.S., et al. *AAPT symposium: Investigating the aging mitigation capabilities of rejuvenators*
575 *in high RAP mixtures using black space diagrams, binder rheology and mixture tests*. in *Asphalt Paving*
576 *Technology: Association of Asphalt Paving Technologists-Proceedings of the Technical Sessions*. 2015.
- 577 50. Gómez-Meijide, B., et al., *Effect of ageing and RAP content on the induction healing properties of asphalt*
578 *mixtures*. Construction and Building Materials, 2018. **179**: p. 468-476.
- 579 51. Airey, G.D., *Rheological properties of styrene butadiene styrene polymer modified road bitumens*. Fuel,
580 2003. **82**(14): p. 1709-1719.
- 581 52. Rahmani, E., et al., *Constitutive modeling of coupled aging-viscoelastic response of asphalt concrete*.
582 Construction and Building Materials, 2017. **131**: p. 1-15.

- 583 53. Liang, Y., et al., *Investigation into the Oxidative Aging of Asphalt Binders*. Transportation Research
584 Record, 2019. **2673**(6): p. 368-378.
- 585 54. Jolliffe, I.T., *Principal Component Analysis*. 2nd ed. Springer series in statistics. Vol. 29. 2002: NY:
586 Springer. 487.
- 587